

1 **Supplementary Materials**

2 **Title: Gut bacterial and fungal communities of the domesticated silkworm**
3 **(*Bombyx mori*) and wild mulberry-feeding relatives**

4

5 Bosheng Chen¹, Kaiqian Du¹, Chao Sun², Arunprasanna Vimalanathan¹, Xili
6 Liang¹, Yong Li³, Baohong Wang⁴, Xingmeng Lu¹, Lanjuan Li⁴ and Yongqi
7 Shao^{1,5,*}

8

9 ¹Institute of Sericulture and Apiculture, College of Animal Sciences, Zhejiang
10 University, Hangzhou, China; ²Analysis Center of Agrobiolgy and
11 Environmental Sciences, Zhejiang University, Hangzhou, China; ³Institute of
12 Soil and Water Resources and Environmental Science, College of
13 Environmental and Resource Sciences, Zhejiang University, Hangzhou, China;
14 ⁴National Collaborative Innovation Center for Diagnosis and Treatment of
15 Infectious Diseases, State Key Laboratory for Diagnosis and Treatment of
16 Infectious Diseases, the First Affiliated Hospital, School of Medicine, Zhejiang
17 University, Hangzhou, China and ⁵Key Laboratory for Molecular Animal
18 Nutrition, Ministry of Education, China

19

20 *Correspondence: Yongqi Shao, E-mail: yshao@zju.edu.cn

21

22 **Supplementary Methods**

23 **Denaturing gradient gel electrophoresis (DGGE)**

24 DGGE investigation of microbiota profile of individual insect and mulberry leaf
25 was performed along with the Illumina MiSeq sequencing (Takano *et al.* 2017,
26 Thompson *et al.* 2008). To amplify the variable V6-V8 region of 16S rRNA gene,
27 PCR was conducted with the primer set 968F-GC-Clamp and 1401R
28 (Supplementary Table S1) under the following conditions: an initial cycle at
29 94 °C for 1 min; 25 cycles at 94 °C for 30 s, 55 °C for 30 s, and 72 °C for 1 min;
30 and a final cycle of 72 °C for 10 min. The 50- μ L PCR mixture contained 2 \times Gflex
31 Buffer (TaKaRa Bio), 0.4 mM dNTP mixture, 0.2 μ M each primer, 1.25 U of Tks
32 Gflex DNA Polymerase, and 2.0 μ L of DNA.

33 DGGE was carried out using the DCode Universal Mutation Detection System
34 (Bio-Rad) onto the 8% polyacrylamide gel with a 20 to 80% denaturant gradient
35 (100% denaturant = 7 M urea and 40% (v/v) deionized formamide). Gels were
36 poured with the aid of a Bio-Rad gradient delivery system. PCR products (~300
37 ng) were electrophoresed in 1 \times TAE buffer (40 mM Tris, 20 mM acetic acid, and
38 1 mM EDTA) at 60 °C for 14 h at 100 V. Gels were stained with SYBR Green I
39 (TaKaRa Bio) for 30 min and then photographed under UV light. DGGE profiles
40 of bacterial 16S rRNA genes were analyzed using Quantity One software
41 (version 4.6.2; Bio-Rad) and BioNumerics software (version 6.01; Applied
42 Maths) as described previously (Chen *et al.* 2016, Lu *et al.* 2013, Thompson *et*

43 *al.* 2008).

44

45 **Illumina sequencing**

46 The V4-V5 region of the eubacteria 16S rRNA gene and the fungal nuclear
47 ribosomal internal transcribed spacer (ITS) region were amplified with primers
48 515F-907R and ITS1F-ITS2, respectively (**Supplementary Table S1**). The
49 sequencing primers contained the adapter and barcode sequences. The PCR
50 reaction was performed in triplicate for each sample. For each reaction, 20 μ L
51 of mixture was prepared, including 5 x FastPfu reaction buffer, 250 μ M dNTPs,
52 1 U FastPfu Polymerase (Transgene, Beijing, China), 200 nM of each primer
53 (Majorbio, Shanghai, China), 1 μ L of template and DNA-free water. The PCR
54 reaction involved a single denaturation step at 95 °C for 3 min, followed by 27
55 cycles of 95 °C for 30 s, 55 °C for 30 s, 72 °C for 45 s, and finished after a
56 final extension at 72°C for 10 min. The triplicate reaction products were pooled
57 and run on a 2% (w/v) agarose gel. Gel fragment of correct size was excised
58 and purified with AxyPrep DNA gel extraction kit (Axygen, Union City, USA).
59 After quantified by Quantifluor dsDNA system (Promega, Madison, USA),
60 products were calculated into equal amount and mixed for Illumina MiSeq (San
61 Diego, CA, USA) paired-end sequencing by a certified sequencing provider
62 (Majorbio, Shanghai, China).

63

64 **Quality filtering and de-multiplexing**

65 The pair-end raw data were initially merged by FLASH (version 1.2.7) (Magoc
66 and Salzberg 2011) with a minimum overlap of 10 base pairs. Merged
67 sequences were trimmed and filtered by Trimmomatic (version 0.36) (Bolger *et*
68 *al.* 2014). Sequences below quality score 20 were end-trimmed to remove low
69 quality nucleotides, and subsequently a 50-nucleotide sliding window scanning
70 from 5' end of read was used to trim group of bases lower than 20 quality score.
71 Sequences lower than 50 bp, primer mismatch >2, barcode mismatch >0 were
72 discarded. According to their unique barcode tags, sequences were
73 demultiplexed for the OTU picking and taxonomic assignment.

74

75 **OTU picking and taxonomic assignment**

76 Sequences passed quality filters were initially taken to identify chimeric
77 sequences by UCHIME algorithm in usearch (version 7.1) (Edgar 2010) with
78 the script *identify_chimeric_seqs.py* implemented in the QIIME software
79 (version 1.8.0) (Caporaso *et al.* 2010). The script *filter_fasta.py* was used for
80 removing chimeric sequences. Afterwards, sequences were clustered into
81 OTUs by usearch with the script *pick_otus.py* with a similarity threshold of 97%.
82 Using the *pick_rep_set.py* script, the most abundant sequence in each OTU
83 cluster was picked as the representative sequence. Representative sequences
84 were classified taxonomically by the script *assign_taxonomy.py* using
85 Greengenes (method, rdp; confidence, 0.80) and Unite database for bacteria
86 and fungi respectively (DeSantis *et al.* 2006, Koljalg *et al.* 2013). To avoid the

87 affection of sequencing depth in difference samples, using the script
88 *single_rarefaction.py* in QIIME, sequences from difference samples were
89 rarefied to the same depth including a large portion of the OTUs and diversity
90 (486 for bacteria DNA data, Good's coverage 94.1%; 612 for bacteria RNA data,
91 Good's coverage 91.7%; and 177 for fungi DNA data, Good's coverage 86.2%),
92 as reported for insects (Yun *et al.* 2014). Rarefaction curve and diversity indices
93 (Sobs, Chao1, ACE, and Shannon) were calculated by 3 steps: First, rarefy
94 OTU table by "multiple_rarefactions.py" with iteration=1000, step=60. The
95 rarefied OTU table generated by random sampling at first step was used for
96 calculating alpha diversity indices by script "alpha_diversity.py". Finally, results
97 of every sample were concatenated into a single file by script "collate_alpha.py".
98 Matrices of weighted and unweighted UniFrac were obtained from the script
99 "beta_diversity.py" with the phylogenetic tree generate by "make_phylogeny.py".

100

101 **Data visualization**

- 102 1. The bar plots of relative abundance of bacteria and fungi in different host
103 species and across different life stages of *B. mori* (Figures 1b, 2a, 4b, 5a
104 and 5b) were visualized by GraphPad Prism (version 6.01) based on the
105 rarefied OTU table, respectively.
- 106 2. The boxplot of bacteria gene copies (Figures 1a, 3a and 4a) was generated
107 by R with the function *geom_boxplot* of the *ggplot2* package (R 2014,
108 Wickham 2016).

109 3. Analysis of alpha diversity estimates and beta diversity indices
110 (**Supplementary Table S3**) were based on the rarefied OTU table. Alpha
111 diversity estimators Ace, Chao, beta diversity indices Shannon, Simpson,
112 and Good's coverage were computed by the *summary.single* command of
113 the mothur software (version 1.30.1) (Schloss *et al.* 2009). The boxplots
114 (Figures 1a, 3b and 4a) showing the species richness and community
115 diversity were based on the OTU number and the Shannon index,
116 respectively, and were visualized by the R package *ggplot2* with the function
117 *geom_boxplot*.

118 4. Considering the large difference in taxon abundance between samples, the
119 PCoA analyses (Figures 1c, 3b, 4d, 5c, 5d) were performed based on the
120 relative abundances of OTUs, and the Bray-Curits distance was calculated
121 using the R package *vegan* with the function *vegdist* and *procomp* (Kelly *et*
122 *al.* 2015, Oksanen *et al.* 2007, Tang *et al.* 2016).

123 5. Heat maps (Figures 1d, 2b, 4e, 5e, 5f) were generated by the R package
124 *vegan* with the function *vegdist* and *hclust*, and the *ggplot2* package with
125 the function *geom_tile*. The Bray-Curits method was used to calculate the
126 distance, followed with Complete-linkage clustering to visualize relationship
127 between samples.

128 6. The Venn diagram (Figure 4c) was based on the OTU list (**Supplementary**
129 **Table S5**), and generated by the R package *VennDiagram* with the function
130 *venn.diagram*.

131

132 **Mothur analysis**

133 Demultiplexed sequences were introduced to Mothur software (Version 1.38.1)
134 (Schloss *et al.* 2009). Sequences were joined into contigs by command
135 “make.contigs” with a list file generated by command “make.file”. Any
136 sequences with ambiguous bases (maxambig=0) and too-long sequences
137 (maxlength=275) were removed by “screen.seqs” command. Afterwards,
138 identical sequences were merged by “unique.seqs” command and aligned
139 against to the Greengenes (Version 13_8) (McDonald *et al.* 2012) or SILVA
140 (Release 128) reference database (Pruesse *et al.* 2007) respectively by
141 “align.seqs” command (we have done both alignments to compare any
142 differences between the two databases used). After removing gap characters
143 (“filter.seqs” command) and duplicate sequences (re-run “unique.seqs”
144 command), the remaining sequences were pre-clustered by command
145 “pre.cluster” with diffs=2. “chimera.uchime” and “remove.seqs” commands
146 were used for identification and removing of chimera sequences (Edgar 2010).
147 The Naïve Bayesian method was used for sequence clustering (Wang *et al.*
148 2007), with Greengenes taxonomy as reference and a bootstrap value of 80%
149 (“classify.seqs” command). Unknown sequences, Archaea sequences,
150 chloroplast sequences, mitochondria sequences were removed by command
151 “remove.lineage”. Cutoff=0.20 was used in the “dist.seqs” command before all
152 sequences clustered into OTU at a divergence of 3% (“cluster.spilt”, taxlevel=4).

153 Phylogenetic tree was generated by FastTree (Version 2.1.3) with generalized
154 time-reversible (GTR) substitution method (Price *et al.* 2010). Each classified
155 OTU was assigned a taxonomy information with command “classify.otu” and
156 binned into phylotypes with the “phylotype” command. For diversity analysis, all
157 samples were normalized by “sub.sample” command to 447 sequences per
158 DNA sample, and 697 sequences per RNA sample, in order to retain more
159 samples. Alpha diversity analysis was performed by command
160 “summary.single”, which generated observed species, Chao1, ace, Shannon
161 indices of each sample. Rarefaction curves were obtained from the command
162 “rarefaction.single”. Bray-Curtis distance matrices used in the heatmap and
163 PCoA analysis were calculated by “dist.shared” command. UniFrac test based
164 on phylogenetic tree was performed by command “unifrac.weighted” and
165 “unifrac.unweighted”. To measure the variation within groups and significance
166 of overall variability between groups, a nonparametric analog of Bartlett’s test
167 for homogeneity of variance, Homogeneity of molecular variance (HOMOVA)
168 (Schloss 2008), was performed by the command “homova”. Variation between
169 different groups in PCoA analysis was calculated by PERMANOVA in R
170 package “vegan”, using the function “adonis”, permutations=999 (Gilleland and
171 Viii 2014).

172 The data produced by Mothur was further compared with that produced by
173 QIIME, based on the OTU table combining the 30 most abundance genera in
174 output of each software. PCoA analysis was based on Bray-Curtis matrices, p-

175 value was calculated by PERMANOVA with permutations=999.

176 **Supplementary Tables**

177 **Supplementary Table S1** Universal primers for the identification of bacteria and fungi.

Primer/Probe	5' modification	Sequence (5' - 3')	Length (bp)	Target	References
27f		AGAGTTTGATCCTGGCTCAG	1465	Bacteria 16S rRNA gene	(Egert <i>et al.</i> 2005)
1492r		GGTTACCTTGTTACGACTT			
ITS1		TCCGTAGGTGAACCTGCGG	Around 700	Fungi ITS (internal transcription spacer) gene	(Anderson and Cairney 2004)
ITS4		TCCTCCGCTTATTGATATGC			
515F		GTGCCAGCMGCCGCGG	392	Bacteria 16S rRNA gene region for Illumina sequencing	(Xiong <i>et al.</i> 2012)
907R		CCGTCAATTCMTTTRAGTTT			
ITS1F		CTTGGTCATTTAGAGGAAGTAA	300	Fungi ITS gene region for Illumina sequencing	(Mukherjee <i>et al.</i> 2014)
ITS2		GCTGCGTTCTTCATCGATGC			
DB200-Qf		CGGYCCAGACTCCTACGGG	200	Quantitative RT PCR	(Lee <i>et al.</i> 1996)
DB200-Qr		TTACCGCGGCTGCTGGCAC			
Wolb-Qf		GCGAAGGCGTCTATCTGGTT	178	Quantitative RT PCR	(This study)
Wolb-Qr		AATCTTGCGACCGTAGTCCC			

968F-GC-Clamp		CGCCCGGGGCGCGCCCGGG CGGGGCGGGGGCACGGGGG AACGCGAAGAACCTTAC	433	Eubacteria	(Shao <i>et al.</i> 2014)
1401Ra		CGGTGTGTACAAGCCCGGGA ACG			
1401Rb		CGGTGTGTACAAGCCCGGGA ACG			

178

179 **Supplementary Table S2** Sequence statistics.

180

	Fungi (DNA-based)	Bacteria (DNA-based)	Bacteria (RNA-based)
Amplified region	ITS1F_2043R	515F_907R	515F_907R
Sample number	9	30	20
Total bases (bp)	287,133,960	749,122,552	438,107,448
Passed QC (bp)	175,515,614	561,640,440	345,957,709
Rate passed QC (%)	61.13	74.97	78.97
Average Length (bp)	306.86	396.47	396.4
Total raw reads	571,980	1,448,300	872,724
Total chloroplast reads	-	1,004,219	420,502
Average reads	63,553	48,277	43,636
Minimum read count	177	31387	29034
Maximum read count	22613	58626	54492
Average reads (chloroplast & mitochondria sequence removed)	-	14,803	11,488
Minimum read count (chloroplast & mitochondria sequence removed)	-	486	612
Maximum read count (chloroplast & mitochondria sequence removed)	-	50887	49473

181

182 **Supplementary Table S3** Diversity metrics across various samples.

183

Sample ID	Reads	0.97					
		OTU	Ace	chao	coverage	Shannon	Simpson
<i>B. mori-1</i>	486	102	167 (137,223)	170 (135,243)	0.8971	3.59 (3.46,3.73)	0.0567 (0.047,0.0664)
<i>B. mori-2</i>	486	80	218 (174,282)	131 (103,193)	0.9156	3.15 (3.01,3.29)	0.091 (0.0763,0.1057)
<i>B. mori-3</i>	486	87	108 -97,132	100 -92,120	0.9465	3.46 (3.33,3.6)	0.0715 (0.0582,0.0848)
<i>D.pyloalis-1</i>	486	49	64 (55,87)	61 (53,88)	0.965	2.19 (2.03,2.35)	0.255 (0.22,0.2901)
<i>D. pyloalis-2</i>	486	50	65 (56,89)	61 (54,82)	0.9609	1.75 (1.58,1.93)	0.4392 (0.3863,0.4921)

			100	98		3.62	0.0441
<i>D. pyloalis-3</i>	486	81	-89,123	-87,125	0.9486	(3.51,3.73)	(0.0375,0.0507)
			40	41		0.41	0.8766
<i>A. major-1</i>	486	19	(25,94)	-25,106	0.9753	(0.29,0.53)	(0.8363,0.9168)
			21	24		0.58	0.8057
<i>A. major-2</i>	486	16	(17,39)	(17,59)	0.9877	(0.45,0.7)	(0.7581,0.8532)
			122	134		2.04	0.2078
Leaf	486	29	-81,195	-68,310	0.9691	(1.92,2.15)	(0.1839,0.2317)

184

185 **Supplementary Table S4** Details of bacterial OTUs shared among *B. mori*, *A.*

186 *major* and *D. pyloalis*.

187

OTU ID	Phylum	Genus
23	Proteobacteria	<i>Pseudomonas</i>
43	Proteobacteria	-
50	Firmicutes	<i>Staphylococcus</i>
177	Proteobacteria	<i>Pseudomonas</i>
435	Firmicutes	<i>Sporolactobacillus</i>
455	Actinobacteria	<i>Rothia</i>
486	Firmicutes	<i>Enterococcus</i>
520	Proteobacteria	<i>Acinetobacter</i>
681	Actinobacteria	<i>Corynebacterium</i>
714	Proteobacteria	<i>Escherichia-Shigella</i>
957	Firmicutes	<i>Allobaculum</i>
1068	Proteobacteria	<i>Pantoea</i>

188

189 **Supplementary Table S5** Details of bacterial OTUs shared across the larval

190 stages of *B. mori*.

191

OTU ID	Phylum	Genus
23	Proteobacteria	<i>Pseudomonas</i>
43	Proteobacteria	-
50	Firmicutes	<i>Staphylococcus</i>
131	Proteobacteria	<i>Sphingomonas</i>
224	Proteobacteria	<i>Acinetobacter</i>
270	Actinobacteria	<i>Rothia</i>
486	Firmicutes	<i>Enterococcus</i>
681	Actinobacteria	<i>Corynebacterium</i>
710	Actinobacteria	<i>Propionibacterium</i>
714	Proteobacteria	<i>Escherichia-Shigella</i>
724	Proteobacteria	-
806	Actinobacteria	<i>Microbacterium</i>
1039	Proteobacteria	<i>Pseudomonas</i>
1068	Proteobacteria	<i>Pantoea</i>

192

193

194 **Supplementary Table S6** HOMOVA analysis across *B. mori* life stages.

195

Group	SSwithin/(Ni-1)	Compare to	p-value
		L2	0.394
		L3	0.397
L1	0.229134	L4	0.300
		L5	0.388
		adult	0.352
		L3	0.104
L2	0.073367	L4	0.106
		L5	0.115
		adult	0.791
		L4	0.798
L3	0.110096	L5	0.292
		adult	0.395
		L5	> 0.999
L4	0.101862	adult	0.397
L5	0.100954	adult	0.378
adult	0.0663201	-	-

196

197

198

199 **Supplementary Table S7** Statistical test for species richness among different

200 Lepidoptera species (one-way ANOVA, LSD post-hoc test).

201

Group1	Group2	Mean difference (I-J)	Std. Error.	Sig.	95% Confidence Interval	
					Lower Bound	Upper Bound
<i>A. major</i>	<i>B. mori</i>	-72.1667*	12.37717	.002**	-103.9832	-40.3501
	<i>D. pyloalis</i>	-42.5000*	12.37717	.019*	-74.3165	-10.6835
<i>B. mori</i>	<i>A. major</i>	72.1667*	12.37717	.002**	40.3501	103.9832
	<i>D. pyloalis</i>	29.6667*	11.07048	.044*	1.2091	58.1242
<i>D. pyloalis</i>	<i>A. major</i>	42.5000*	12.37717	.019*	10.6835	74.3165
	<i>B. mori</i>	-29.6667*	11.07048	.044*	-58.1242	-1.2091

202 * : $P \leq 0.05$, ** : $P \leq 0.01$

203 **Supplementary Table S8** PERMANOVA test based on distance matrices.

204

Test	Sample group	Value	Bray-Curtis	Weighted UniFrac	Unweighted UniFrac
PERMANOVA ("adonis")	RNA: <i>B. mori</i> early-instar vs. late-instar	R2 p	0.2959 <0.001**	0.29398 <0.001**	0.18967 <0.001**
	RNA: domesticated silkworm vs. wild Lepidoptera insects	R2 p	0.401661 0.041*	0.39017 0.034*	0.3233 0.011*
	DNA: <i>B. mori</i> early-instar vs. late-instar	R2 p	0.42206 <0.001**	0.41705 <0.001**	0.09134 0.008**
	DNA: domesticated silkworm vs. wild Lepidoptera insects	R2 p	0.40079 0.019**	0.28072 0.1	0.25725 0.028*

Foregut vs. Midgut	R2	0.24993	0.28198	0.20074
	p	0.4	0.3	0.9
Foregut vs. Hindgut	R2	0.34755	0.35081	0.51186
	p	0.6667	0.6667	0.1
Midgut vs. Hindgut	R2	0.28567	0.32796	0.24206
	p	0.4	0.3	1

205 **Supplementary Table S9** Statistical test for species richness among different
 206 gut regions (one-way ANOVA, LSD post-hoc test).

Group1	Group2	Mean difference (I-J)	Std. Error.	Sig.	95% Confidence Interval	
					Lower Bound	Upper Bound
	Hindgut	33.0000	25.77359	.248	-30.0657	96.0657
Foregut	Midgut	26.5000	23.52796	.303	-31.0708	84.0708
	Whole gut	16.8333	23.52796	.501	-40.7375	74.4042
	Foregut	-33.0000	25.77359	.248	-96.0657	30.0657
Hindgut	Midgut	-6.5000	23.52796	.792	-64.0708	51.0708
	Whole gut	-16.1667	23.52796	.518	-73.7375	41.4042
	Foregut	-26.5000	23.52796	.303	-84.0708	31.0708
Midgut	Hindgut	6.5000	23.52796	.792	-51.0708	64.0708
	Whole gut	-9.6667	21.04405	.662	-61.1596	41.8263
	Foregut	-16.8333	23.52796	.501	-74.4042	40.7375
Whole gut	Hindgut	16.1667	23.52796	.518	-41.4042	73.7375
	Midgut	9.6667	21.04405	.662	-41.8263	61.1596

207

208 **Supplementary Table S10** Statistical test for species richness across *B. mori*

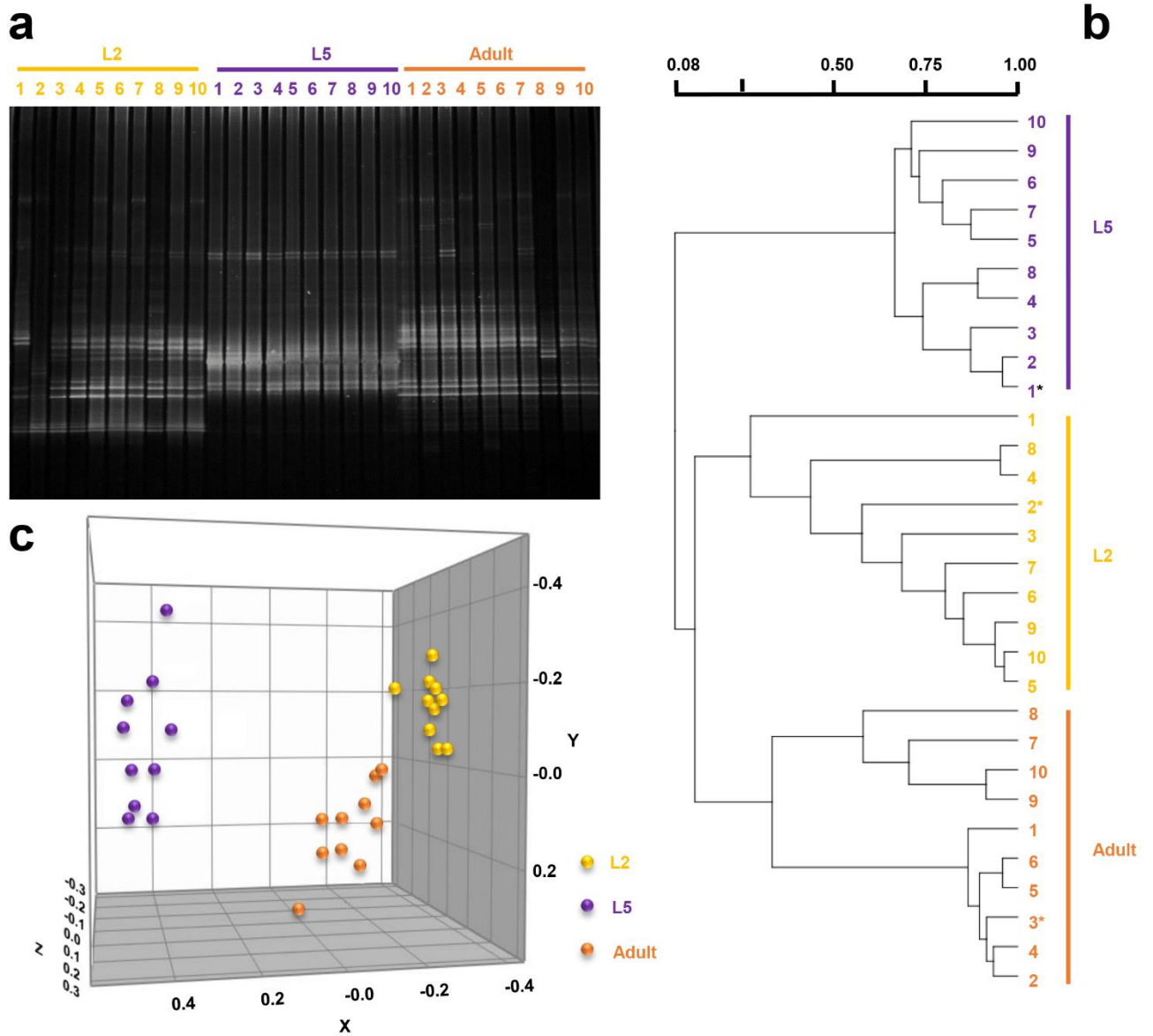
209 life stages (one-way ANOVA, LSD post-hoc test).

Group1	Group2	Mean difference (I-J)	Std. Error.	Sig.	95% Confidence Interval	
					Lower Bound	Upper Bound
L1	L2	-44.6667*	11.68332	.003**	-70.6987	-18.6346
	L3	-30.0000*	11.68332	.028*	-56.0321	-3.9679
	L4	-39.6667*	11.68332	.007**	-65.6987	-13.6346
	L5	-60.6667*	11.68332	.000**	-86.6987	-34.6346
	adult	-43.0000*	12.79844	.007**	-71.5167	-14.4833
L2	L1	44.6667*	11.68332	.003**	18.6346	70.6987
	L3	14.6667	10.44988	.191	-8.6171	37.9505
	L4	5.0000	10.44988	.643	-18.2838	28.2838
	L5	-16.0000	10.44988	.157	-39.2838	7.2838
	adult	1.6667	11.68332	.889	-24.3654	27.6987
L3	L1	30.0000*	11.68332	.028*	3.9679	56.0321
	L2	-14.6667	10.44988	.191	-37.9505	8.6171
	L4	-9.6667	10.44988	.377	-32.9505	13.6171
	L5	-30.6667*	10.44988	.015*	-53.9505	-7.3829
	adult	-13.0000	11.68332	.292	-39.0321	13.0321
L4	L1	39.6667*	11.68332	.007**	13.6346	65.6987
	L2	-5.0000	10.44988	.643	-28.2838	18.2838

	L3	9.6667	10.44988	.377	-13.6171	32.9505
	L5	-21.0000	10.44988	.072	-44.2838	2.2838
	adult	-3.3333	11.68332	.781	-29.3654	22.6987
	L1	60.6667*	11.68332	.000**	34.6346	86.6987
	L2	16.0000	10.44988	.157	-7.2838	39.2838
L5	L3	30.6667*	10.44988	.015*	7.3829	53.9505
	L4	21.0000	10.44988	.072	-2.2838	44.2838
	adult	17.6667	11.68332	.161	-8.3654	43.6987
	L1	43.0000*	12.79844	.007**	14.4833	71.5167
	L2	-1.6667	11.68332	.889	-27.6987	24.3654
adult	L3	13.0000	11.68332	.292	-13.0321	39.0321
	L4	3.3333	11.68332	.781	-22.6987	29.3654
	L5	-17.6667	11.68332	.161	-43.6987	8.3654

210 * : $P \leq 0.05$, ** : $P \leq 0.01$

211 **Supplementary Figures**



212

213 **Supplementary Figure S1** DGGE analyses of PCR-amplified 16S rRNA gene

214 fragments of bacterial communities across silkworm life-stage. (a) DGGE

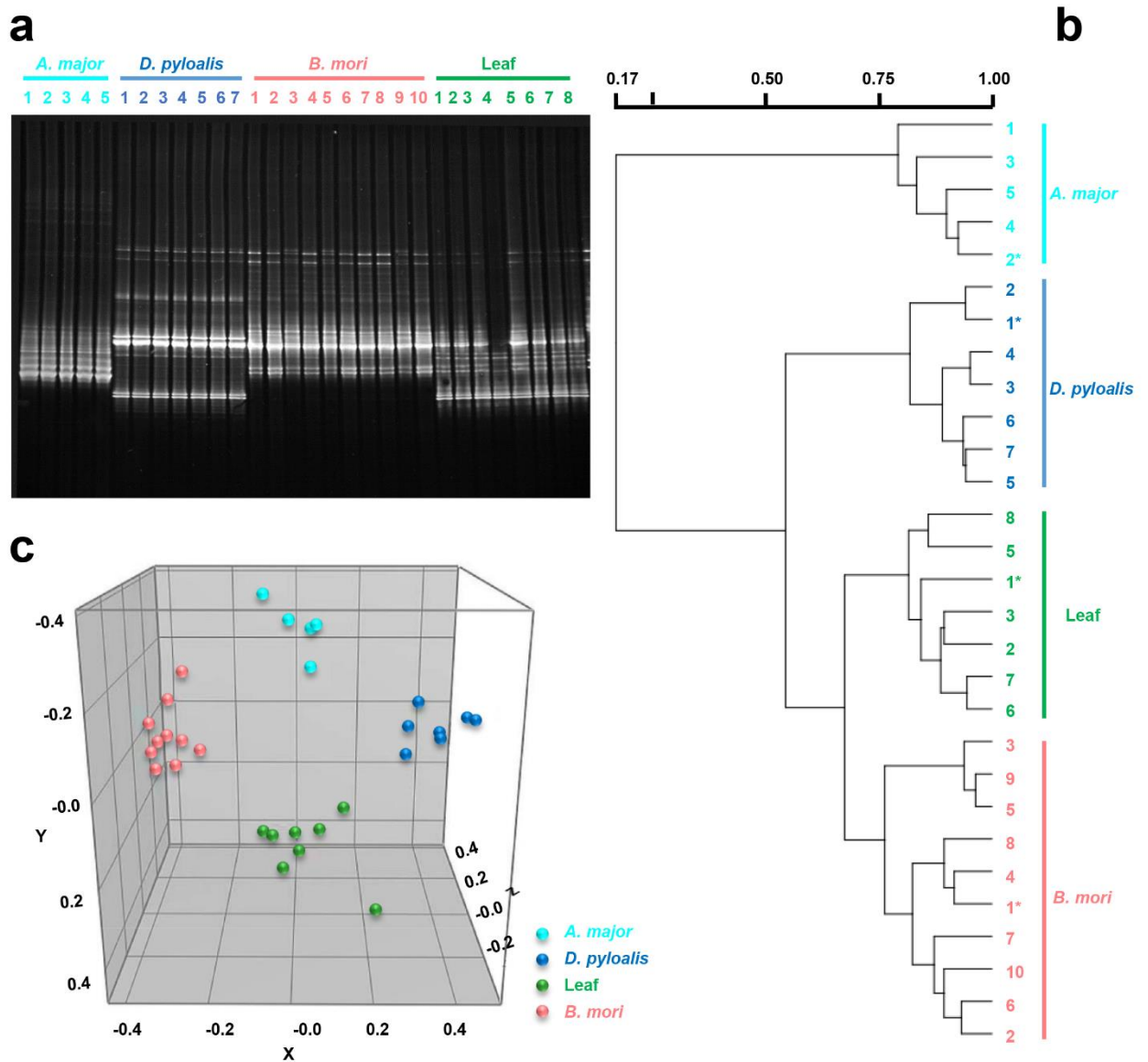
215 patterns of the early-instar (L2) and late-instar (L5) larval gut microbiota and

216 adult gut microbiota of different individuals. (b) Dendrogram of community

217 DGGE fingerprint similarities. Dendrogram was constructed by the unweighted

218 pair group method using arithmetic averages (UPGMA). (c) Multidimensional

219 scaling (MDS) analysis of the cluster shown in (b). MDS is an optimized 3D
220 representation of the similarity matrix, and these similarities were calculated as
221 a best estimate using the Euclidean distance between two gel lanes (points in
222 the MDS plot) to provide a convenient visual interpretation. The X-, Y-, and Z-
223 axes separately represent three different dimensions: Dim 1, Dim 2, and Dim 3.
224 According to the plot, individual samples (same color key) of each life-stage
225 were grouped together, which suggested the uniqueness and stability of the
226 predominant microbiota composition of each individual. *, represents the MiSeq
227 sequencing sample.



228

229 **Supplementary Figure S2** DGGE analyses of PCR-amplified 16S rRNA gene

230 fragments of bacterial communities associated with mulberry-feeding

231 Lepidoptera insects and mulberry leaves. (a) DGGE patterns of the final instar

232 larval gut microbiotas of *A. major*, *D. pyloalis* and *B. mori*, and microbiota

233 associated with mulberry leaves. (b) Dendrogram of community DGGE

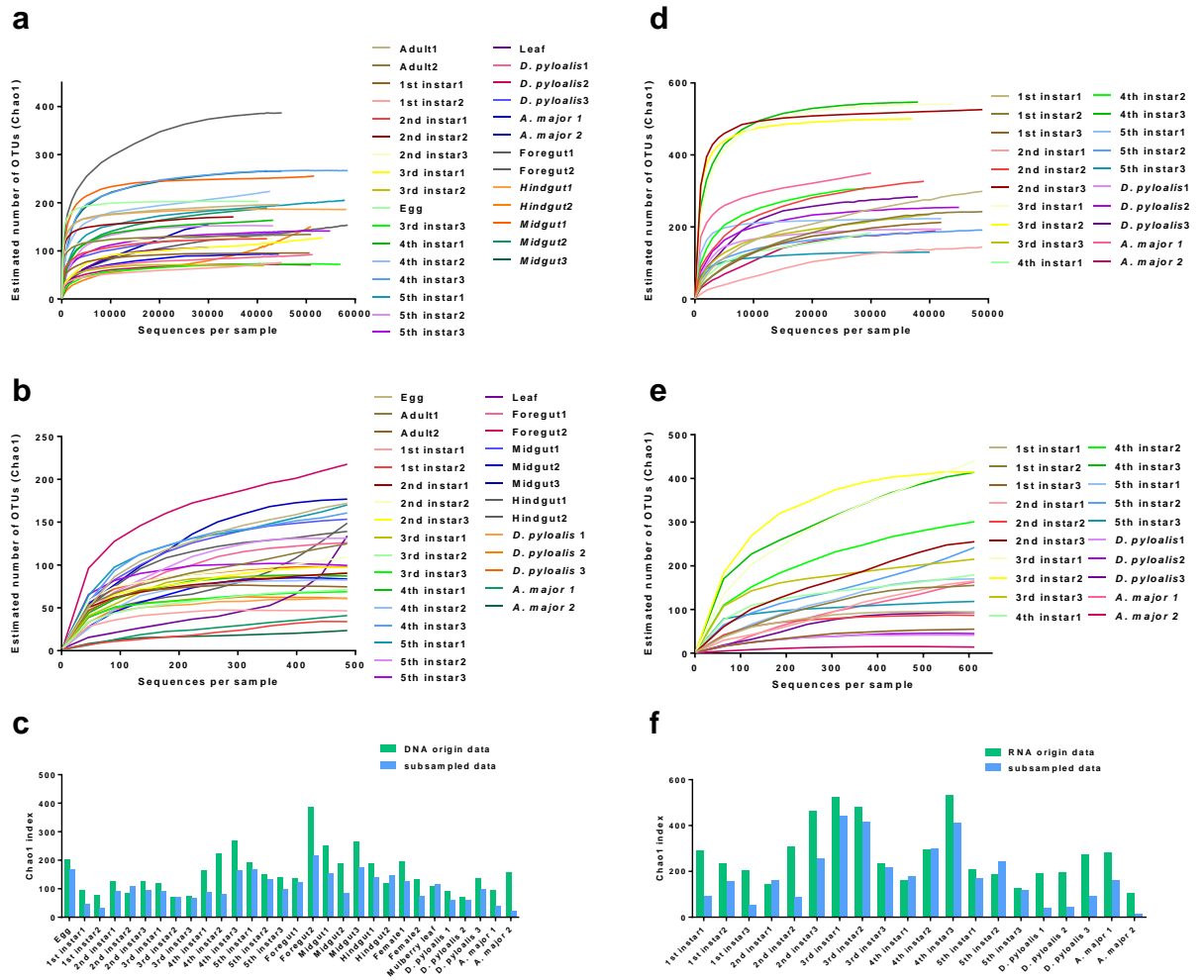
234 fingerprint similarities. Dendrogram was constructed by the unweighted pair

235 group method using arithmetic averages (UPGMA). (c) Multidimensional

236 scaling (MDS) analysis of the cluster shown in (b). MDS is an optimized 3D

237 representation of the similarity matrix, and these similarities were calculated as
238 a best estimate using the Euclidean distance between two gel lanes (points in
239 the MDS plot) to provide a convenient visual interpretation. The X-, Y-, and Z-
240 axes separately represent three different dimensions: Dim 1, Dim 2, and Dim 3.
241 According to the plot, individual samples (same color key) of each host species
242 were grouped together, which suggested the uniqueness and stability of the
243 predominant microbiota composition of each individual. *, represents the MiSeq
244 sequencing sample.

245



246

247 **Supplementary Figure S3** Rarefaction curves depicted from original

248 sequencing data sets and randomly subsampled data sets with the same

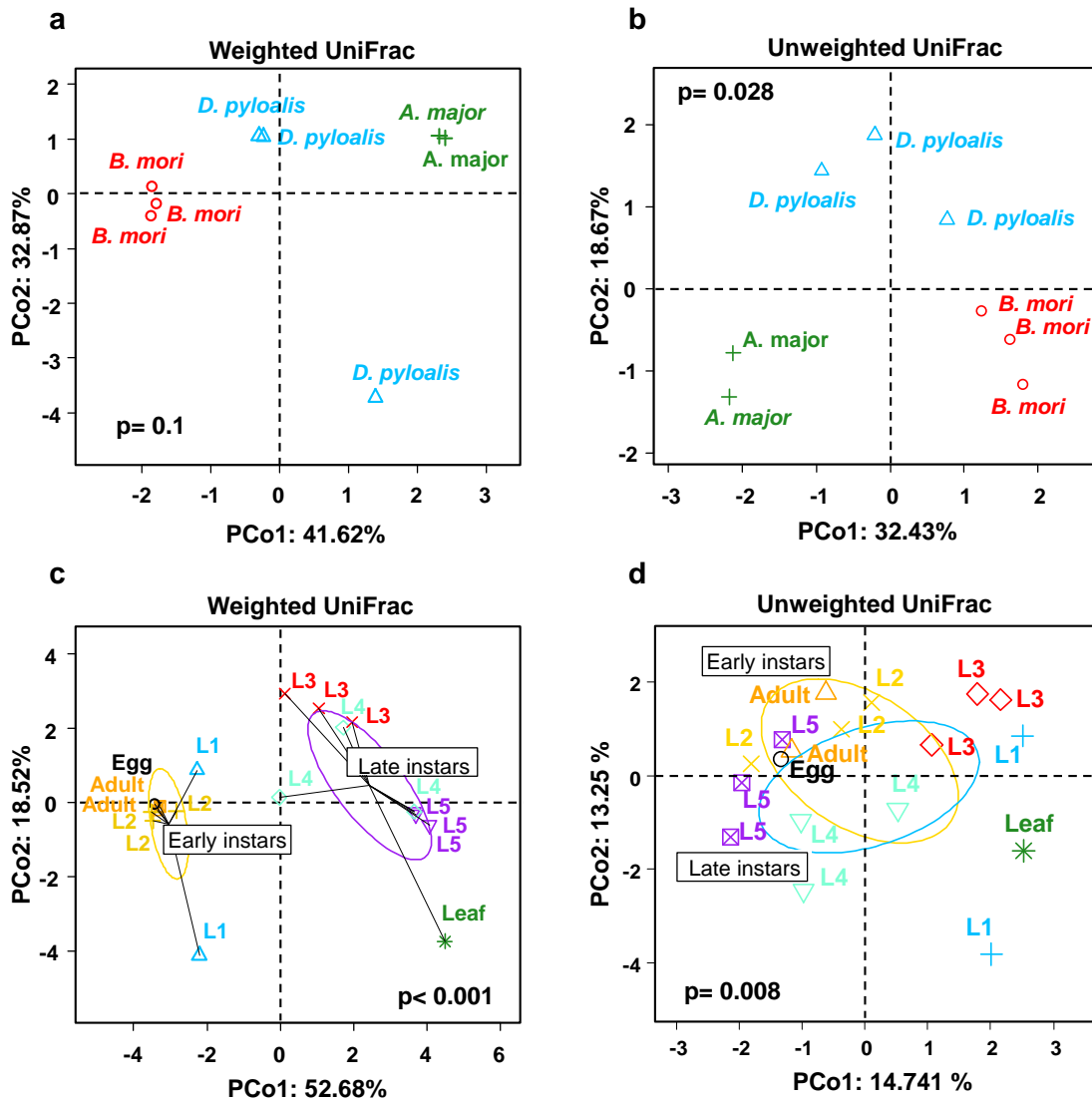
249 number of 16S sequences. (a) and (d), rarefaction curves of original DNA and

250 RNA sequencing samples. (b) and (e), rarefaction curves of subsampled DNA

251 (486) and RNA (612) sequences. Comparison of species richness between

252 original and subsampled sequencing data was shown in (c) DNA samples and

253 (f) RNA samples. Diversity index was calculated with 1000 iteration.



254

255 **Supplementary Figure S4** PCoA analysis of DNA sequencing samples. (a)

256 PCoA plot using weighted and (b) unweighted UniFrac distance between

257 Lepidoptera species. (c) PCoA plot using weighted and (d) unweighted UniFrac

258 distance across *B. mori* life-stage. PERMANOVA was used for significance

259 analysis, permutation=999.

260

261

262

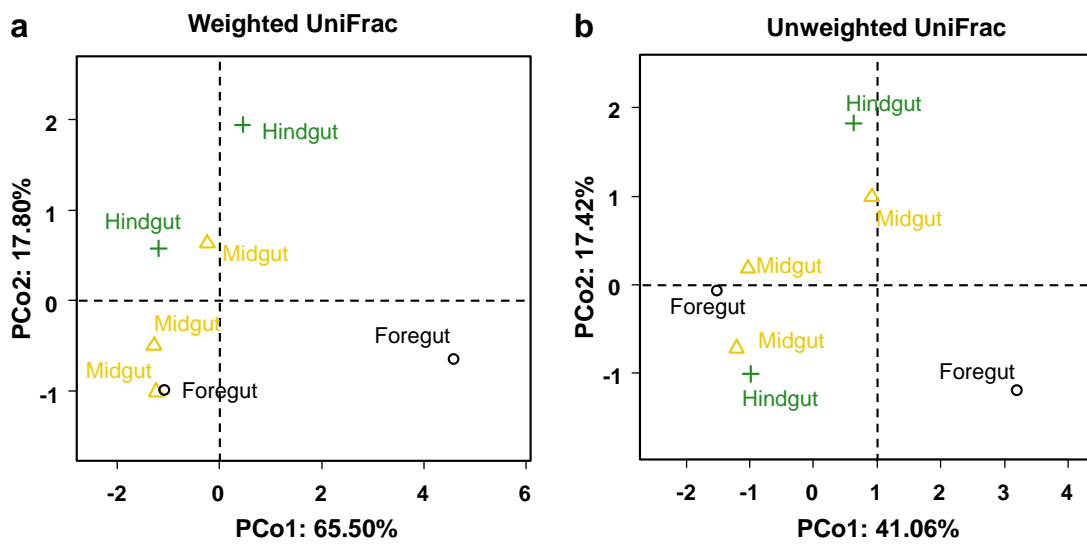
263

264

265

266

267



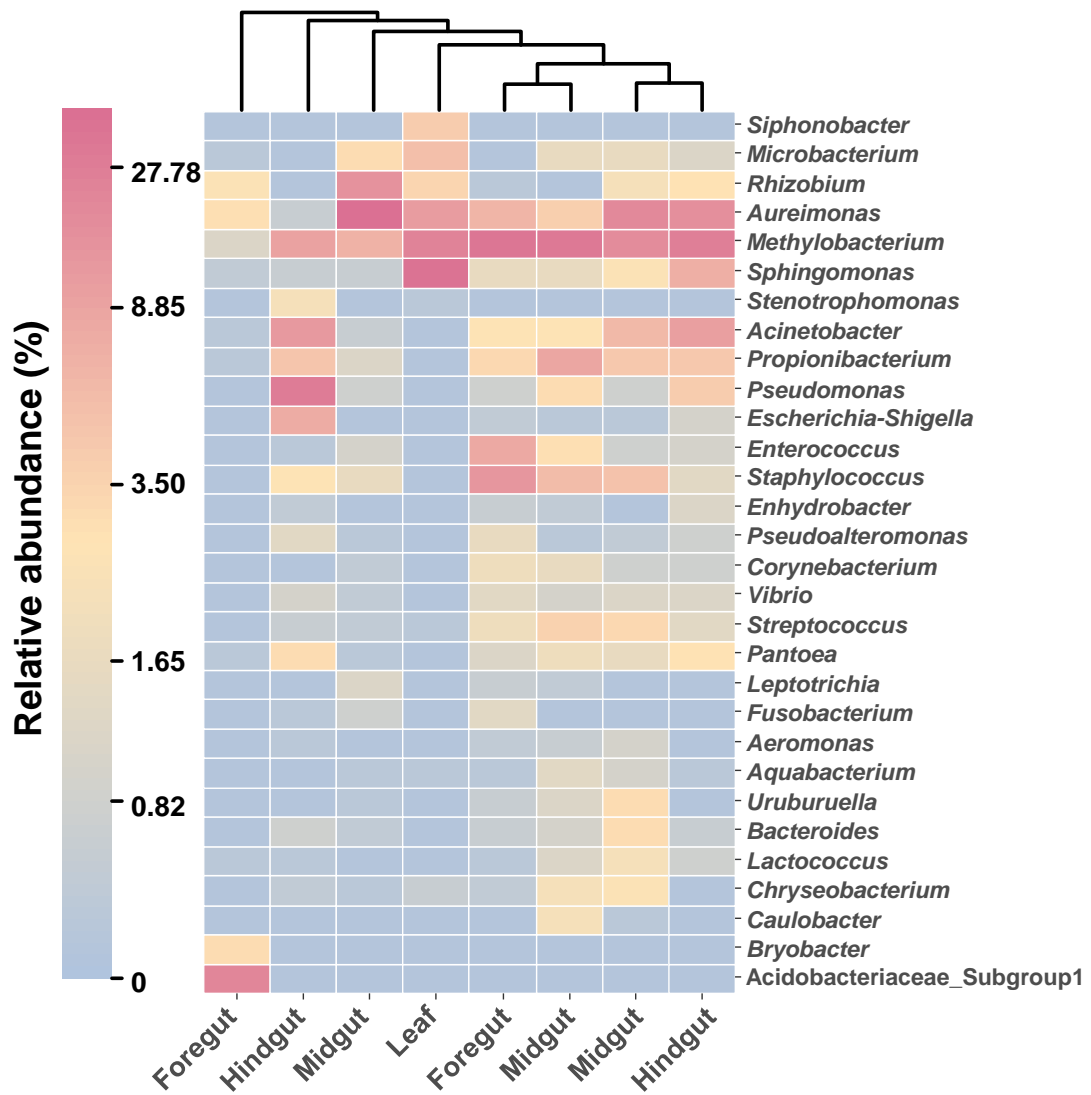
268

269 **Supplementary Figure S5** PCoA analysis of gut regions. (a) PCoA plot using

270 weighted and (b) unweighted UniFrac distance between gut regions.

271 PERMANOVA was used for significance analysis, permutation=999, $P > 0.05$.

272



273

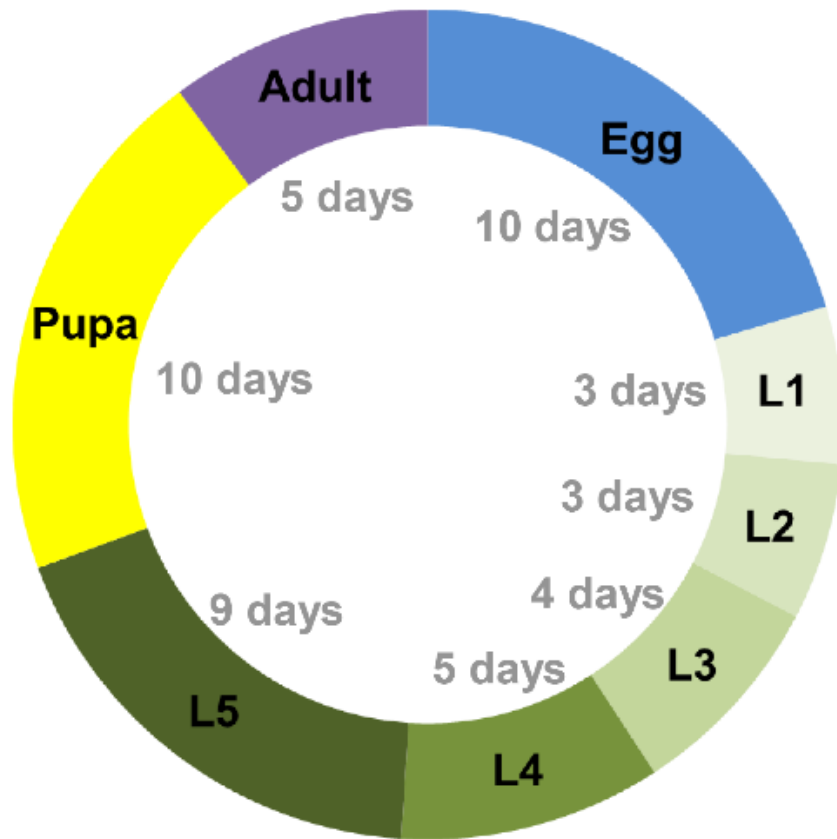
274 **Supplementary Figure S6** Clustering analysis of dominant gut bacteria in

275 different gut regions of the 5th-instar *B. mori*. Relative abundances of the 30

276 most abundant genera are shown in a heatmap, with cluster analysis using

277 Bray-Curtis distance, followed by a complete-linkage method.

278



279

280 **Supplementary Figure S7** *Bombyx mori* life cycle.

281

282

283

284

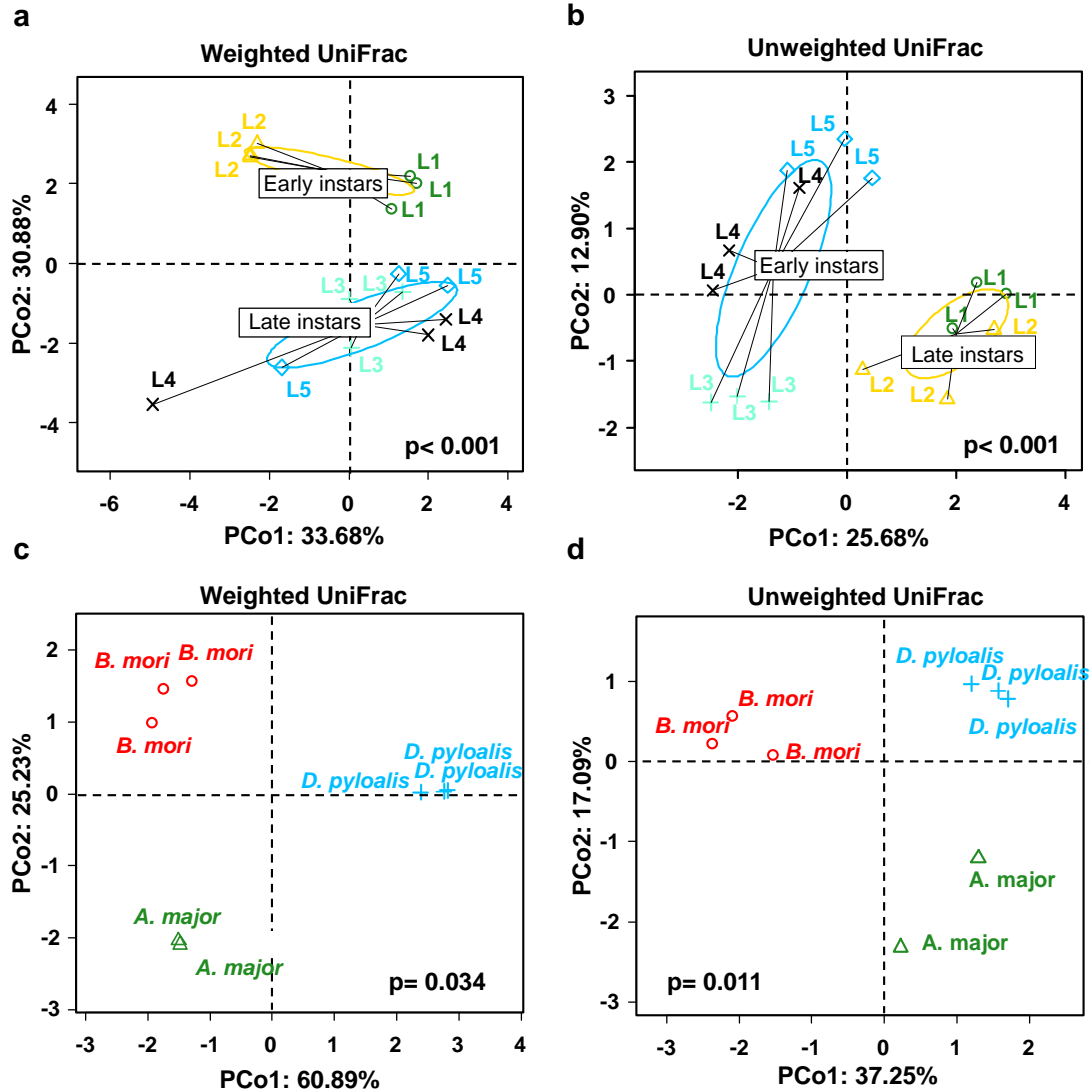
285

286

287

288

289



290

291 **Supplementary Figure S8** PCoA analysis of RNA sequencing samples. (a)

292 PCoA plot using weighted and (b) unweighted UniFrac distance across *B. mori*

293 life-stage. (c) PCoA plot using weighted and (d) unweighted UniFrac distance

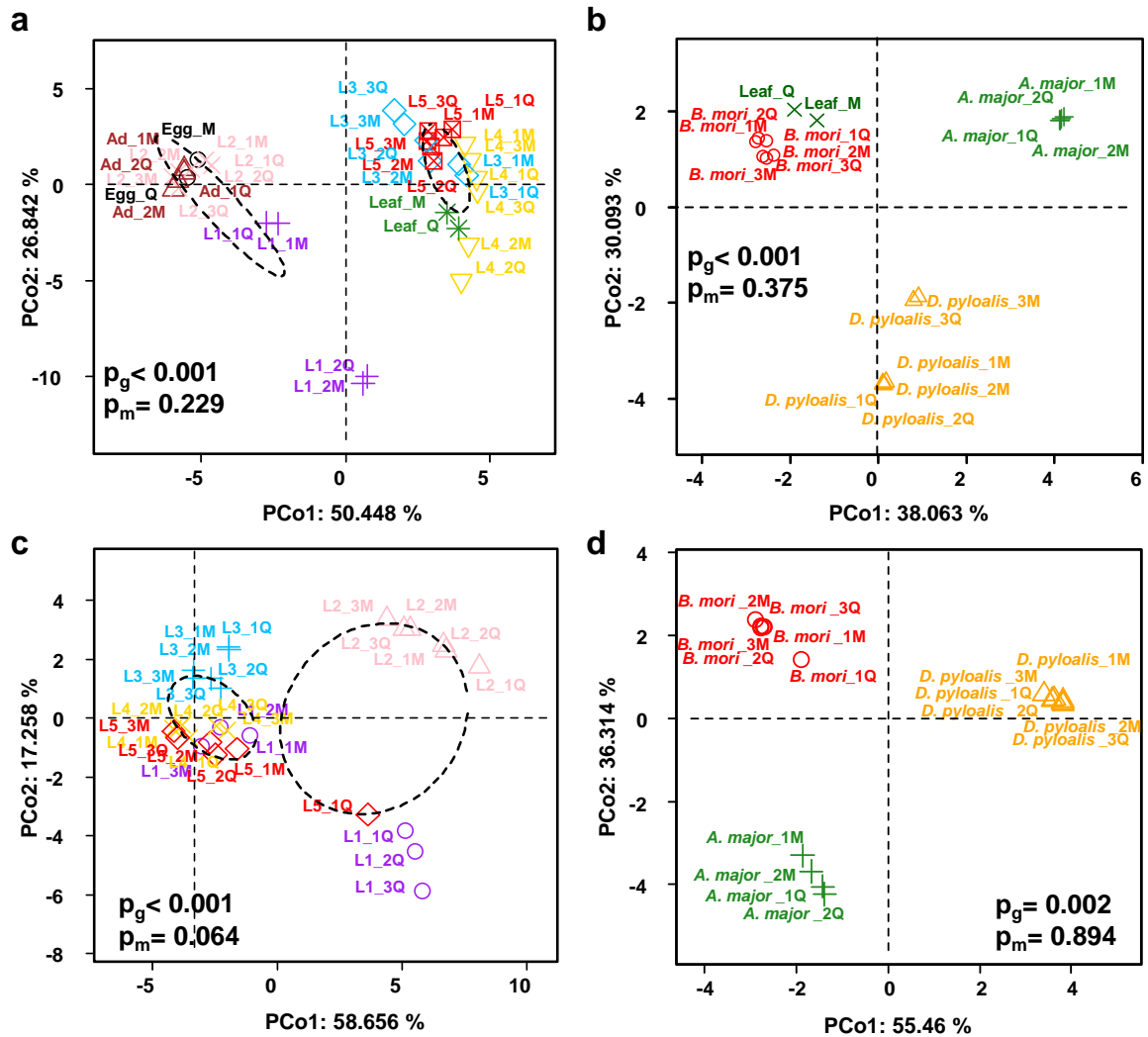
294 between Lepidoptera species. PERMANOVA was used for significance

295 analysis, permutation=999.

296

297

298



299

300 **Supplementary Figure S9** Comparison of sequencing results analyzed by
 301 mothur and by QIIME. (a) PCoA plot using Bray–Curtis distances across *B. mori*
 302 life-stage and (b) between Lepidoptera species in DNA sequencing samples.
 303 (c) PCoA plot using Bray–Curtis distances across *B. mori* life-stage and (d)
 304 between Lepidoptera species in RNA sequencing samples. Bray-Curtis matrix
 305 was generated from the OTU table combining the 30 most abundant genera
 306 from QIIME and mothur, respectively. M, represents data extracted from mothur;
 307 Q, from QIIME. P value, calculated by PERMANOVA at 999 permutation. Pg, P

308 value of group variation between life-stage (a, c) or host species (b, d). Pm, P
309 value of method variation between mothur and QIIME analysis.

310

311 **References**

312 Anderson IC, Cairney JW (2004). Diversity and ecology of soil fungal
313 communities: increased understanding through the application of
314 molecular techniques. *Environ Microbiol* **6**: 769–779.

315

316 Bolger AM, Lohse M, Usadel B (2014). Trimmomatic: a flexible trimmer
317 for Illumina sequence data. *Bioinformatics* **30**: 2114–2120.

318

319 Caporaso JG, Kuczynski J, Stombaugh J, Bittinger K, Bushman FD,
320 Costello EK *et al.* (2010). QIIME allows analysis of high-throughput
321 community sequencing data. *Nat Methods* **7**: 335–336.

322

323 Chen B, Teh BS, Sun C, Hu S, Lu X, Boland W *et al.* (2016). Biodiversity
324 and activity of the gut microbiota across the life history of the
325 insect herbivore *Spodoptera littoralis*. *Sci Rep* **6**: 29505.

326

327 DeSantis TZ, Hugenholtz P, Larsen N, Rojas M, Brodie EL, Keller K *et*
328 *al.* (2006). Greengenes, a chimera-checked 16S rRNA gene database and
329 workbench compatible with ARB. *Appl Environ Microbiol* **72**: 5069–5072.

330

331 Edgar RC (2010). Search and clustering orders of magnitude faster than
332 BLAST. *Bioinformatics* **26**: 2460–2461.

333

334 Egert M, Stingl U, Bruun LD, Pommerenke B, Brune A, Friedrich MW (2005).
335 Structure and topology of microbial communities in the major gut
336 compartments of *Melolontha melolontha* larvae (Coleoptera:
337 Scarabaeidae). *Appl Environ Microbiol* **71**: 4556–4566.

338

339 Gilleland E, Viii G (2014). R Development Core Team (2008). R: A
340 language and environment for statistical computing. R Foundation for
341 Statistical Computing.

342

343 Kelly BJ, Gross R, Bittinger K, Sherrill-Mix S, Lewis JD, Collman RG
344 *et al.* (2015). Power and sample-size estimation for microbiome studies

345 using pairwise distances and PERMANOVA. *Bioinformatics* **31**: 2461–2468.
346
347 Koljalg U, Nilsson RH, Abarenkov K, Tedersoo L, Taylor AF, Bahram M *et*
348 *al.* (2013). Towards a unified paradigm for sequence-based
349 identification of fungi. *Mol Ecol* **22**: 5271–5277.
350
351 Lee DH, Zo YG, Kim SJ (1996). Nonradioactive method to study genetic
352 profiles of natural bacterial communities by PCR-single-strand-
353 conformation polymorphism. *Appl Environ Microbiol* **62**: 3112–3120.
354
355 Lu H, He J, Wu Z, Xu W, Zhang H, Ye P *et al.* (2013). Assessment of
356 microbiome variation during the perioperative period in liver
357 transplant patients: a retrospective analysis. *Microbial Ecol* **65**: 781–
358 791.
359
360 Magoc T, Salzberg SL (2011). FLASH: fast length adjustment of short
361 reads to improve genome assemblies. *Bioinformatics* **27**: 2957–2963.
362
363 McDonald D, Price MN, Goodrich J, Nawrocki EP, DeSantis TZ, Probst A
364 *et al.* (2012). An improved Greengenes taxonomy with explicit ranks for
365 ecological and evolutionary analyses of bacteria and archaea. *ISME J*
366 **6**: 610–618.
367
368 Mukherjee PK, Chandra J, Retuerto M, Sikaroodi M, Brown RE, Jurevic R
369 *et al.* (2014). Oral mycobiome analysis of HIV-infected patients:
370 identification of *Pichia* as an antagonist of opportunistic fungi. *PLoS*
371 *Pathog* **10**: e1003996.
372
373 Oksanen J, Kindt R, Legendre P, O’ Hara B, Stevens MHH, Oksanen MJ *et*
374 *al.* (2007). The vegan package. *Community ecology package* **10**: 631–637.
375
376 Price MN, Dehal PS, Arkin AP (2010). FastTree 2—approximately maximum-
377 likelihood trees for large alignments. *PLoS One* **5**: e9490.
378
379 Pruesse E, Quast C, Knittel K, Fuchs BM, Ludwig W, Peplies J *et al.*
380 (2007). SILVA: a comprehensive online resource for quality checked and
381 aligned ribosomal RNA sequence data compatible with ARB. *Nucleic Acids*
382 *Res* **35**: 7188–7196.
383
384 R (2014). R: A language and environment for statistical computing.
385 Vienna, Austria: R Foundation for Statistical Computing; 2014.
386
387 Schloss PD (2008). Evaluating different approaches that test whether
388 microbial communities have the same structure. *ISME J* **2**: 265–275.

389
390 Schloss PD, Westcott SL, Ryabin T, Hall JR, Hartmann M, Hollister EB
391 *et al.* (2009). Introducing mothur: open-source, platform-independent,
392 community-supported software for describing and comparing microbial
393 communities. *Appl Environ Microbiol* **75**: 7537–7541.
394
395 Shao Y, Arias-Cordero E, Guo H, Bartram S, Boland W (2014). In vivo
396 Pyro-SIP assessing active gut microbiota of the cotton leafworm,
397 *Spodoptera littoralis*. *PLoS One* **9**: e85948.
398
399 Takano SI, Tuda M, Takasu K, Furuya N, Imamura Y, Kim S *et al.* (2017).
400 Unique clade of alphaproteobacterial endosymbionts induces complete
401 cytoplasmic incompatibility in the coconut beetle. *Proc Natl Acad Sci*
402 *U S A* **114**: 6110–6115.
403
404 Tang ZZ, Chen G, Alekseyenko AV (2016). PERMANOVA-S: association test
405 for microbial community composition that accommodates confounders and
406 multiple distances. *Bioinformatics* **32**: 2618–2625.
407
408 Thompson CL, Wang B, Holmes AJ (2008). The immediate environment during
409 postnatal development has long-term impact on gut community structure
410 in pigs. *ISME J* **2**: 739–748.
411
412 Wang Q, Garrity GM, Tiedje JM, Cole JR (2007). Naive Bayesian
413 classifier for rapid assignment of rRNA sequences into the new
414 bacterial taxonomy. *Appl Environ Microbiol* **73**: 5261–5267.
415
416 Wickham H (2016). *ggplot2: elegant graphics for data analysis*. Springer.
417
418 Xiong J, Liu Y, Lin X, Zhang H, Zeng J, Hou J *et al.* (2012). Geographic
419 distance and pH drive bacterial distribution in alkaline lake sediments
420 across Tibetan Plateau. *Environ Microbiol* **14**: 2457–2466.
421
422 Yun JH, Roh SW, Whon TW, Jung MJ, Kim MS, Park DS *et al.* (2014). Insect
423 gut bacterial diversity determined by environmental habitat, diet,
424 developmental stage, and phylogeny of host. *Appl Environ Microbiol* **80**:
425 5254–5264.
426